Cosco, Francesco; Maniscalco, Sabrina

Memory effects in a quasiperiodic Fermi lattice

Published in:
Physical Review A

DOI:
10.1103/PhysRevA.98.053608

Published: 05/11/2018

Document Version
Publisher's PDF, also known as Version of record

Please cite the original version:
Cosco, F., & Maniscalco, S. (2018). Memory effects in a quasiperiodic Fermi lattice. Physical Review A, 98(5), 1-6. [053608]. https://doi.org/10.1103/PhysRevA.98.053608

Memory effects in a quasiperiodic Fermi lattice

Francesco Cosco[1] and Sabrina Maniscalco[1,2]
[1]*QTF Centre of Excellence, Turku Centre for Quantum Physics, Department of Physics and Astronomy, University of Turku, FI-20014 Turun yliopisto, Finland*
[2]*QTF Centre of Excellence, Department of Applied Physics, Aalto University, FI-00076 Aalto, Finland*

(Received 11 September 2018; published 5 November 2018)

We investigate a system of fermions trapped in a quasiperiodic potential from an open quantum system theory perspective, designing a protocol in which an impurity atom (a two-level system) is coupled to a trapped fermionic cloud described by the noninteracting Aubry-André model. The Fermi system is prepared in a charge-density-wave state before it starts its relaxation. In this work we focus our attention on the time evolution of the impurity in such an out-of-equilibrium environment and study whether the induced dynamics can be classified as Markovian or non-Markovian. We find how the localized phase of the Aubry-André model displays evidence of strong and stable memory effects and can be considered as a controllable and robust non-Markovian environment.

DOI: 10.1103/PhysRevA.98.053608

I. INTRODUCTION

A great deal of attention has been devoted to quasiperiodic systems, described by Aubry-André (AA) -type Hamiltonians [1]. These models have been often compared to Anderson insulating systems for their ability of displaying similar localization phenomena but in a controllable way. In fact, the localization in the AA model is fully deterministic, making quasiperiodic geometries intrinsically different from true disordered systems [2]. Experimentally, AA models can be created by a combination of two periodic functions having incommensurate wave numbers. A bichromatic optical lattice designed in such a way allows one to realize a quasiperiodic geometry for a trapped gas in a cold-atom setup [3]. In this system, the interplay between the quasiperiodic potential and the kinetic energy rules the metal-to-insulator transition [4,5].

The high level of tunability and control of the strength and shape of the external potentials forming the bichromatic lattice makes these setups a unique candidate to explore a series of interesting physical phenomena. Recently, interacting fermions trapped in quasiperiodic optical lattices were used to observe effects of many-body localization and ergodicity breaking. Specifically, using initial high-energy states with strong charge-density-wave order, i.e., an initial state with particles occupying exclusively odd or even sites, it has been shown how the relaxation properties of such a system vary in the presence of a quasiperiodic engineered on-site potential. In particular, it has been observed how the crossover from ergodic to nonergodic dynamics can be witnessed by monitoring the density imbalance in the occupation of even and odd sites at long times [6,7].

Furthermore, this system has been drawing attention as an interesting setup in which to study impurity dynamics. In [8] it was shown how, when adiabatically perturbed by local perturbations, a nonlocal-density rearrangement occurs. This allowed to introduce the concept of statistical orthogonality catastrophe [9,10]. In [11] the effect of a sudden local perturbation was used to characterize time irreversibility, and the decay of the Loschmidt echo of the Fermi gas was found to be exponential or algebraic in the two phases of the AA model. In this last example the system was prepared in the charge-density-wave state before introducing the impurity potential. We are here interested in describing the AA model from an open quantum system theory perspective: We consider the fermions trapped in the quasiperiodic optical lattice to act as an environment for an embedded impurity. In this paper we link the open dynamics of the impurity to the Loschmidt echo of the gas but, instead of examining properties such as long-time dynamics and functional decay of the echo itself, we aim at understanding whether the open dynamics of the impurity can be classified as Markovian or non-Markovian. Our aim is to explore the emergence of memory effects and see whether a Markovian–to–non-Markovian crossover witnesses the metal-to-insulator transition typical of the AA model.

Recent investigations of lattice systems as an environment for impurities have looked, directly or indirectly, to the connection between non-Markovian effects and localization in two very different setups. In [12] it was shown, for example, that for a system of coupled cavities with random disorder the non-Markovian character of the open system dynamics increases monotonically as the disorder is increased. In this setup the localization phenomenon is exactly Anderson localization, and for nonzero disorder the dynamics is found to be always non-Markovian. On the other hand, in [13] a perturbed Bose-Hubbard lattice was investigated, showing how the superfluid–to–Mott-insulator transition roughly corresponds to a Markovian–to–non-Markovian crossover. In that work, however, the onset of memory effects and the critical point do not coincide exactly. Rather, the onset of non-Markovianity signals a change in how the information travels through the quenched lattice. These works establish a connection between memory effects and localization phenomena, in the former case originated by a potential and in the latter induced by the interaction between the bosons. By using as the environment the AA model and its unique features, we aim to gain insight into the connection between non-Markovianity and localization. When compared with the Bose-Hubbard model, where the parameter driving the superfluid–to–Mott-insulator transition is the interaction between the bosons, we expect that, in an experimentally realistic scenario, the quasiperiodic potential may display a higher level of controllability. When compared with the one-dimensional Anderson insulator, the main advantage is the existence of a well-defined critical (nonzero) point in the metal-to-insulator transition.

For its experimental and fundamental interest we assume our environment to be a fermionic system prepared in a charge-density-wave state, before embedding the impurity in the lattice. In general, fermionic baths are much less explored environments in the open quantum system community and, conceptually, since the environment is not initially prepared in an eigenstate, this scenario allows us to explore the dynamics of an open system interacting with an out-of-equilibrium environment, which will evolve even in the absence of the impurity. In this context, deriving a master equation is a challenging task, but we overcome this limit by focusing our studies on noninteracting fermions. This allow us to compute exactly and efficiently the dynamics of the open system through determinant formulas. Our work can be framed within the quantum probing paradigm, whose basic idea is the extraction of relevant information about a many-body system by monitoring the time evolution of an embedded impurity. In this framework the impurity acts as readout device and permits, in principle, one to extract information about the many-body nature of the environment by measurements performed exclusively on the open system. So far many protocols have been proposed to probe trapped cold atoms with quantum impurities, for example, protocols that use the impurities as thermometers [14] or to measure quantum correlations in bosonic systems [15], and to probe the orthogonality catastrophe in trapped fermion environments [16–20].

The paper is organized as follows. In Sec. II we introduce the microscopic model considered: We describe in detail the Aubry-André Hamiltonian, the impurity, and the impurity-fermion interaction. We define our figure of merit, i.e., the Loschmidt echo of the trapped Fermi gas and the non-Markovianity measure. Throughout this work we quantify memory effects through the measure proposed by Breuer *et al.* [21]. This measure is defined in terms of the amount of information backflow, i.e., the information that travels back from the environment to the open system during the dynamics. We then show how the exact solution for the time evolution of the impurity can be computed in terms of a determinant formula, i.e., the Levitov formula. In Sec. III we study the Loschmidt echo, describe its behavior for different values of the quasiperiodic potential, and quantify the memory effects related to the open dynamics of the impurity. We discuss the role of the lattice size, of the effective strength of the impurity-fermion interaction, and of the phase factor present in the quasiperiodic potential. Finally, in Sec. IV we summarize our findings and show how the insulating phase is a source of dominant and robust memory effects.

II. MODEL, PROTOCOL, AND METHODS

A one-dimensional gas of atoms trapped in a bichromatic optical potential confined to the lowest Bloch band can be described by the tight-binding Hamiltonian

$$\hat{H}_{AA} = -J\sum_{i=1}(\hat{a}^{\dagger}_{i+i}\hat{a}_i + \hat{a}^{\dagger}_i\hat{a}_{i+1}) + \Delta\sum_{i=1}\cos(2\pi\beta i+\phi)\hat{a}^{\dagger}_i\hat{a}_i \tag{1}$$

in which J is the hopping parameter, Δ is the the strength of the on-site potential, β is the ratio between the frequencies of the two optical potentials generating the lattice, and $\hat{a}_i$ and $\hat{a}^{\dagger}_i$ are standard fermionic ladder operators. The hopping parameter and the localizing potential can be derived from the local forces and potentials acting on the atoms [22]. This model is known as the Aubry-André Hamiltonian. It has been proven that, for irrational β, i.e., when the on-site potential is quasiperiodic, at $\Delta > 2J$ the model shows a transition from delocalized to localized single-particle eigenstates.

Here we aim at using a single atomic impurity to explore the features of the model in its two phases, the delocalized one and the localized one. We assume the impurity to be placed in a site of the bichromatic optical lattice, say, $i = x$, and coupled to the lattice gas through a density-density interaction, which couples the internal levels of the impurity to the local number operator $\hat{n}_x$. Furthermore, we assume that only the two lowest internal levels of the impurity contribute to the dynamics, labeling them $|e\rangle$ and $|g\rangle$, and that $|g\rangle$ is transparent to the gas. The interaction Hamiltonian reads, under these assumptions,

$$\hat{H}_{\rm int} = \epsilon|e\rangle\langle e|\otimes\hat{a}^{\dagger}_x\hat{a}_x, \tag{2}$$

in which ϵ is an effective coupling constant. The chosen form of the interaction Hamiltonian in Eq. (2) guarantees that the evolution of the impurity is a purely dephasing dynamics, i.e.,

$$\hat{\rho}_S(t) = \Lambda_t[\hat{\rho}_S(0)] = {\rm Tr}[\hat{U}(t)\rho_S(0)\otimes\rho_E(0)\hat{U}^{\dagger}(t)] = \begin{pmatrix}\rho_{gg}(0) & \chi^*(t)\rho_{ge}(0)\\ \chi(t)\rho_{eg}(0) & \rho_{ee}(0)\end{pmatrix}, \tag{3}$$

where $\hat{\rho}_S(0)$ and $\hat{\rho}_E(0)$ are the initial states of impurity and environment, respectively, which are assumed to be initially uncorrelated. By means of the Levitov formula [23] we can write the time evolution of the off-diagonal element of the reduced density matrix of the impurity as

$$\chi(t) = \det(1-\hat{r}+\hat{r}e^{-i\hat{h}_e t}e^{i\hat{h}_g t}), \tag{4}$$

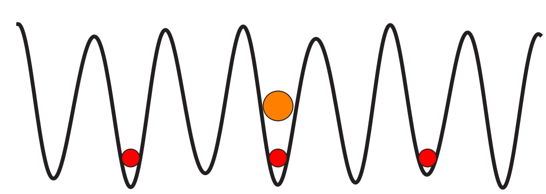

FIG. 1. Sketch of an impurity atom (orange) embedded in a trapped Fermi lattice (red). At $t = 0$ the gas is prepared in the so-called charge-density-wave state in which they occupy only odd (or even) lattice sites.

where $\hat{r}$ is a single-particle operator depending on the specific choice of the initial state of the fermionic environment and $\hat{h}_{e\,(g)}$ is the single-particle counterpart of $\hat{H}_{e\,(g)} = \langle e\ (g)|\hat{H}_{AA} + \hat{H}_{\text{int}}|e\ (g)\rangle$.

Several measures or witnesses of non-Markovianity, based on different properties, have been proposed and employed in the attempt to define and quantify memory effects [24–29]. In this work we follow the framework set by Breuer *et al.*, which identifies non-Markovianity with information flowing from the environment to the open system [21]. This measure is built considering how the distinguishability between two quantum states evolves in time under the effect of a dynamical map. Distinguishability is defined here through trace distance that, for two generic quantum states $\hat{\rho}_1$ and $\hat{\rho}_2$, reads $D(\hat{\rho}_1, \hat{\rho}_2) \equiv \frac{1}{2}\text{Tr}\sqrt{(\hat{\rho}_1 - \hat{\rho}_2)(\hat{\rho}_1 - \hat{\rho}_2)}$, and is contractive under completely positive and trace-preserving maps. Variations in the distinguishability are associated with a flow of information between the open system and the environment. If the distinguishability decreases, the information is flowing from the open system to the environment; if the distinguishability increases, some information, previously lost to the environment, is flowing back to the open system. In a Markovian process, the distinguishability can only decrease, monotonically, as a function of time, signaling a loss of information, with information flowing exclusively to the environment. Breuer *et al.* in [21] identified a partial and temporary increase in trace distance with non-Markovian dynamics. Consequently, the non-Markovianity measure is defined as

$$\mathcal{N}[\Lambda] = \max_{\rho_{1,2}(0)} \int_{\dot{D}>0} dt \left[\frac{d}{dt} D(\Lambda_t \hat{\rho}_1(0), \Lambda_t \hat{\rho}_2(0))\right], \qquad (5)$$

which is often referred to as information backflow. In the case of a two-level system undergoing a dephasing dynamics, the maximization over the optimal pair of initial states appearing in Eq. (5) can be carried out analytically. It can be shown that the optimal pair of states satisfies the relations $[\hat{\rho}_1(0) - \hat{\rho}_2(0)]_{gg} = 0$ and $|[\hat{\rho}_1(0) - \hat{\rho}_2(0)]_{eg}|^2 = 1$ [30]. With these conditions it is straightforward to show that the optimized trace distance is given by the absolute value of the decoherence function

$$D_{\text{opt}}(t) = |\chi(t)|. \qquad (6)$$

With the ultimate goal of probing the fermionic environment, we can design a Ramsey-type interferometric protocol in which we assume the total initial state to be initially factorized as $\rho(0) = |\psi\rangle\langle\psi| \otimes |\Phi\rangle\langle\Phi|$, with $|\Phi\rangle$ being the initial state of the fermionic gas and $|\psi\rangle = \frac{1}{\sqrt{2}}(|g\rangle + |e\rangle)$ the initial state of the impurity. In this case the Loschmidt echo $L(t)$ of the Fermi gas and the off-diagonal element of the impurity reduced density matrix $\chi(t)$ are simply related by

$$\sqrt{L(t)} = |\chi(t)| = |\langle\Phi|e^{-i\hat{H}_e t} e^{i\hat{H}_g t}|\Phi\rangle|. \qquad (7)$$

In the following we consider the initial state of the fermionic environment to be the so-called charge-density-wave state, in which only even or odd sites are initially populated by the fermions of the environment. Choosing to populate the odd

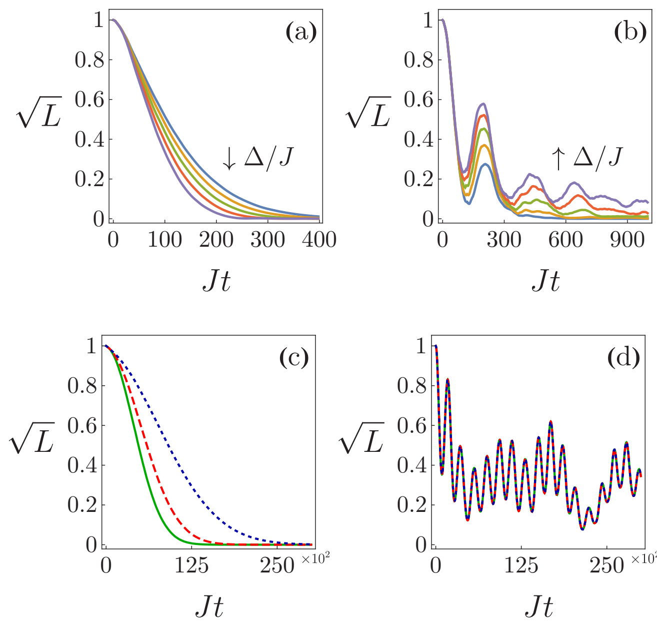

FIG. 2. Square root of the Loschmidt echo for different system parameters: (a) $\Delta/J = 1.5$, 1.55, 1.6, 1.65, and 1.7 from blue to purple, respectively, and (b) $\Delta/J = 2.03$, 2.08, 2.13, 2.18, and 2.23 from blue to purple, respectively. In (a) and (b) $L = 233$ and $\epsilon/J = 10^{-1}$ are used. (c) Square root of the Loschmidt echo for $\Delta/J = 0.5$ for three different sizes $L = 233$, 377, and 987 in solid green, dashed red, and dotted blue lines, respectively. (d) Square root of the Loschmidt echo for $\Delta/J = 2.5$ for three different sizes $L = 233$, 377, and 987 in green, red, and blue, respectively. In (c) and (d) $\epsilon/J = 10^{-2}$.

sites, the initial state of the Fermi gas can be written as

$$|\Phi\rangle = \prod_{i\ \text{odd}} \hat{a}_i^\dagger |0\rangle, \qquad (8)$$

where $|0\rangle$ represents the vacuum state. Contrarily to the usual assumption in open quantum system theory the initial state of the environment is not an eigenstate of the unperturbed Hamiltonian and will evolve in time even without the impurity (a sketch of the setup is provided in Fig. 1). In this situation, deriving a master equation by standard techniques is a rather challenging task. However, the coherences of the impurity can be computed exactly and efficiently from the determinant formula introduced in Eq. (4) as

$$\chi(t) = \det(1 - \hat{n}_{\text{CDW}} + \hat{n}_{\text{CDW}} e^{-i\hat{h}_e t} e^{i\hat{h}_g t}), \qquad (9)$$

where $\hat{n}_{\text{CDW}} = \sum_{i\ \text{odd}} |i\rangle\langle i|$. The information backflow associated with this time evolution, combining Eqs. (5)–(7), is

$$\mathcal{N}_- = \sum_n \sqrt{L(t_{2n})} - \sqrt{L(t_{1n})}, \qquad (10)$$

where $[t_{1n}, t_{2n}]$ are the time intervals over which $\sqrt{L}$ increases. Notice that we have included a minus sign subscript to highlight that during these time intervals some of the previously lost information regarding the state of the impurity is temporarily recovered. In the same fashion, summing instead over the time intervals in which $\sqrt{L}$ decreases, we can define the information outflow $\mathcal{N}_+$, i.e., the information that flows

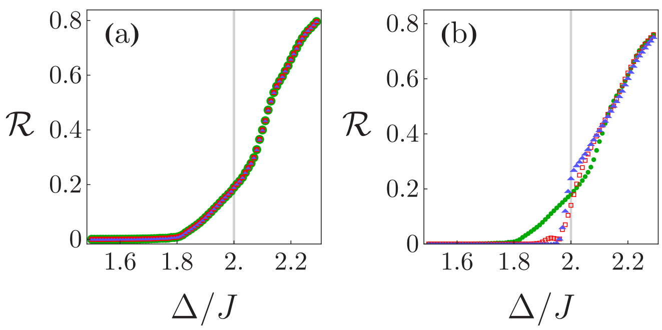

FIG. 3. (a) Plot of $\mathcal{R}$ as a function of Δ/J with $\epsilon/J = 10^{-1}$. The green circles, red squares, and blue triangles correspond to the results for $L = 233$, 377, and 987, respectively. (b) Plot of $\mathcal{R}$ for a fixed size $L = 233$ with different impurity-fermion coupling, namely, $\epsilon/J = 10^{-1}$, 10^{-2}, and 10^{-3} for the green circles, red squares, and blue triangles, respectively. The vertical lines in (a) and (b) are at $\Delta/J = 2$.

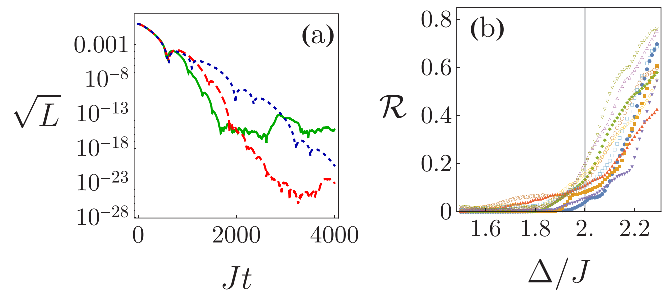

FIG. 4. (a) Square root of the Loschmidt echo, shown in logarithmic scale, for $\Delta/J = 1.5$ for three different sizes $L = 233$, 377, and 987 in solid green, dashed red, and dotted blue lines, respectively. (b) Ratio between information backflow and information outflow as a function of the ratio Δ/J. Ten random values of the phase ϕ have been used and they correspond to the different colors and shapes. In both (a) and (b) $\epsilon/J = 10^{-1}$. The vertical line in (b) is at $\Delta/J = 2$.

from the system to the environment. In what follows we consider a normalized version of the non-Markovianity measure in Eq. (5), defined as the ratio between the information backflow and the information outflow:

$$\mathcal{R} = \frac{\mathcal{N}_-}{\mathcal{N}_+}. \tag{11}$$

The non-Markovianity quantifier defined in this way is naturally bounded between zero and one.

III. RESULTS

In this section we show how, tracking the time evolution of the impurity coherences and quantifying the information backflow, the Fermi gas can act as a tunable environment where the amount of memory effects is determined by the strength of the quasiperiodic on-site potential. We take β to be the golden ratio, i.e., $\beta = \frac{1+\sqrt{5}}{2}$, and the lattice length L to coincide with a number from the Fibonacci sequence. With this choice for the size of the lattice we can impose periodic boundary conditions and avoid effects due to the interaction of the impurity with edge states. We fix the position of the impurity to be $x = 1$ and consider the sums in the Hamiltonian of Eq. (1) to run from $i = -\frac{L-1}{2}$ to $i = \frac{L-1}{2}$. Where not specified otherwise, we consider the phase factor $\phi = 0$.

In Fig. 2 we start off by displaying the square root of the Loschmidt echo and show how it qualitatively changes as a function of the lattice parameters. In Figs. 2(a) and 2(b) we keep fixed the lattice size $L = 377$ and the fermion-impurity coupling $\epsilon/J = 10^{-1}$ and change the strength of the on-site potential. By varying Δ/J we can study how the response of the trapped gas changes in the two phases of the Aubry-André model. The two phases are indeed found to give rise to very different behaviors for the Loschmidt echo. In the delocalized phase, displayed in Fig. 2(a), the Loschmidt echo appears to decay in time without displaying any appreciable structure in the timescale considered. In this regime the decay gets faster and faster as the ratio Δ/J is increased. In the localized phase, displayed in Fig. 2(b), the decay of the Loschmidt echo appears to be suppressed for stronger values of the quasiperiodic potential and displays a series of clear and strong oscillations. As anticipated, revivals in the coherences of the open system undergoing a dephasing time evolution are signals of non-Markovian dynamics and memory effects. In the two phases the dependence of the behavior of Loschmidt echo from the system size is also dramatically different. In the delocalized phase, displayed in Fig. 2(c), the Loschmidt echo decays on longer timescales when the lattice size is increased. On the other hand, in the localized phase, displayed in Fig. 2(d), the Loschmidt echo appears to be size independent as expected for a localized system.

To summarize these findings we now quantify the memory effects characterizing the impurity dynamics through the non-Markovianity measure defined in Eq. (11). The behavior of the normalized information backflow $\mathcal{R}$, illustrated in Fig. 3(a), shows that in the localized phase of the Aubry-André model, the impurity dynamics is clearly strongly non-Markovian. However, for these values of the parameters, the metal-to-insulator transition of the Aubry-André model does not coincide with the Markovian–to–non-Markovian crossover. This result appears to be effectively independent of the lattice size, as shown in the same figure. Interestingly, however, a greater role is played by the coupling between the fermions and the impurity. In fact, when reducing this interaction strength, the rise of strong memory effects shifts towards the critical point of the Aubry-André model. This is shown in Fig. 3(b), where the normalized information backflow $\mathcal{R}$ signals a sharper separation between the delocalized phase and the localized phase, as we decrease the values of the fermion-impurity interaction. In other words, the delocalized phase is extremely sensitive to small perturbations and already for small values of the probe-environment coupling memory effects occur. However, a sharp increase in $\mathcal{R}$ occurs at the metal-insulator transition point in the weak-coupling regime, as shown in Fig. 3(b) by blue triangles. These memory effects appear also to be robust and stable in the localized phase in the sense that for different couplings the ratio between information backflow and information outflow, after the critical point, reaches comparable values.

It is important to stress that we are not claiming that the impurity dynamics in the delocalized phase of the AA model is fully Markovian; in fact, in Fig. 4(a) we show the Loschmidt echo of the Fermi lattice for $\Delta/J = 1.5$ and even in this case we can witness some revivals. However, the resulting information backflow is found to be several orders of magnitude lower than the information outflow, making it very difficult to detect in a feasible experimental scenario. Moreover, it is strongly dependent on the lattice size. We conjecture, however, that in the weak probe-environment coupling regime and in the thermodynamic limit, the information backflow will vanish.

To conclude our analysis we finally briefly discuss the role of the phase factor ϕ appearing in the on-site potential of the Aubry-André Hamiltonian. In Fig. 4(b) the non-Markovianity quantifier $\mathcal{R}$ is displayed for a set of random values of the phase factor ϕ. The effect of different phase factors is to shift randomly the rise of strong non-Markovianity in the critical region close to $\Delta/J = 2$. For some values of the phase factor the onset moves farther from the critical point, while for others it moves toward it. Nevertheless, the trend appears to be similar after the metal-to-insulator transition with the ratio between information backflow and information outflow increasing as the quasiperiodic potential is increased as well.

IV. CONCLUSION

Our results contribute to the exploration of the possible connection between the presence of memory effects in the impurity dynamics and localization in the environment. We cannot claim that the Markovian–to–non-Markovian crossover, which we demonstrate occurs in this system, coincides with the metal-to-insulator transition typical of the Aubry-André model. Nevertheless, the two phases of the Aubry-André model induce very different behaviors in the impurity dynamics as witnessed by the Loschmidt echo, for an initial charge-density-wave state of the Fermi gas. When the environment is in the delocalized phase, we witness indeed negligible oscillations (from a realistic experimental perspective) and a strong dependence on the system parameters, such as the lattice length, the impurity–Fermi-gas coupling, and the phase factor present in the quasiperiodic potential. In the localized phase of the environment, for $\Delta/J > 2$, the impurity dynamics is instead characterized by strong and robust non-Markovian effects. In this region the ratio between information backflow and information outflow becomes incredibly stable against the system parameters. In particular, it is size independent, as it is also the Loschmidt echo in this regime, and varying the coupling between the impurity and the trapped fermions does not affect considerably the non-Markovianity quantifier. These findings make the Aubry-André Fermi lattice an ideal candidate for a tunable fermionic environment, allowing us to investigate fundamental phenomena of open quantum systems dynamics in a controlled way and using a nontrivial environment model.

ACKNOWLEDGMENTS

The authors acknowledge financial support from the Horizon 2020 EU collaborative project QuProCS (Grant Agreement No. 641277), the Academy of Finland Centre of Excellence program (Project No. 312058), and the Academy of Finland (Project No. 287750).

[1] S. Aubry and G. André, Ann. Isr. Phys. Soc. **3**, 18 (1980).

[2] P. W. Anderson, Phys. Rev. **109**, 1492 (1958).

[3] G. Roati, C. D'Errico, L. Fallani, M. Fattori, C. Fort, M. Zaccanti, G. Modugno, M. Modugno, and M. Inguscio, Nature (London) **453**, 895 (2008).

[4] D. J. Thouless and Q. Niu, J. Phys. A: Math. Gen. **16**, 1911 (1983).

[5] M. Modugno, New J. Phys. **11**, 033023 (2009).

[6] P. Bordia, H. Lüschen, S. Scherg, S. Gopalakrishnan, M. Knap, U. Schneider, and I. Bloch, Phys. Rev. X **7**, 041047 (2017).

[7] H. P. Lüschen, P. Bordia, S. Scherg, F. Alet, E. Altman, U. Schneider, and I. Bloch, Phys. Rev. Lett. **119**, 260401 (2017).

[8] V. Khemani, R. Nandkishore, and S. L. Sondhi, Nat. Phys. **11**, 560 (2015).

[9] D.-L. Deng, J. H. Pixley, X. Li, and S. Das Sarma, Phys. Rev. B **92**, 220201 (2015).

[10] F. Cosco, M. Borrelli, E.-M. Laine, S. Pascazio, A. Scardicchio, and S. Maniscalco, New J. Phys. **20**, 073041 (2018).

[11] S. Vardhan, G. De Tomasi, M. Heyl, E. J. Heller, and F. Pollmann, Phys. Rev. Lett. **119**, 016802 (2017).

[12] S. Lorenzo, F. Lombardo, F. Ciccarello, and G. M. Palma, Sci. Rep. **7**, 42729 (2017).

[13] F. Cosco, M. Borrelli, J. J. Mendoza-Arenas, F. Plastina, D. Jaksch, and S. Maniscalco, Phys. Rev. A **97**, 040101 (2018).

[14] T. H. Johnson, F. Cosco, M. T. Mitchison, D. Jaksch, and S. R. Clark, Phys. Rev. A **93**, 053619 (2016).

[15] T. J. Elliott and T. H. Johnson, Phys. Rev. A **93**, 043612 (2016).

[16] J. Goold, T. Fogarty, N. Lo Gullo, M. Paternostro, and T. Busch, Phys. Rev. A **84**, 063632 (2011).

[17] M. Knap, A. Shashi, Y. Nishida, A. Imambekov, D. A. Abanin, and E. Demler, Phys. Rev. X **2**, 041020 (2012).

[18] A. Sindona, J. Goold, N. Lo Gullo, S. Lorenzo, and F. Plastina, Phys. Rev. Lett. **111**, 165303 (2013).

[19] M. Cetina, M. Jag, R. S. Lous, I. Fritsche, J. T. M. Walraven, R. Grimm, J. Levinsen, M. M. Parish, R. Schmidt, M. Knap, and E. Demler, Science **354**, 96 (2016).

[20] R. Schmidt, M. Knap, D. A. Ivanov, J.-S. You, M. Cetina, and E. Demler, Rep. Prog. Phys. **81**, 024401 (2018).

[21] H.-P. Breuer, E.-M. Laine, and J. Piilo, Phys. Rev. Lett. **103**, 210401 (2009).

[22] J. Settino, N. Lo Gullo, A. Sindona, J. Goold, and F. Plastina, Phys. Rev. A **95**, 033605 (2017).

[23] I. Klich, in *Quantum Noise in Mesoscopic Physics*, edited by Y. V. Nazarov (Springer Netherlands, Dordrecht, 2003), pp. 397–402.

[24] A. Rivas, S. F. Huelga, and M. B. Plenio, Phys. Rev. Lett. **105**, 050403 (2010).

[25] S. Luo, S. Fu, and H. Song, Phys. Rev. A **86**, 044101 (2012).

[26] S. Lorenzo, F. Plastina, and M. Paternostro, Phys. Rev. A **88**, 020102 (2013).

[27] N. Lo Gullo, I. Sinayskiy, T. Busch, and F. Petruccione, arXiv:1401.1126.

[28] B. Bylicka, D. Chruściński, and S. Maniscalco, Sci. Rep. **4**, 5720 (2014).

[29] F. A. Pollock, C. Rodríguez-Rosario, T. Frauenheim, M. Paternostro, and K. Modi, Phys. Rev. Lett. **120**, 040405 (2018).

[30] H.-P. Breuer, E.-M. Laine, J. Piilo, and B. Vacchini, Rev. Mod. Phys. **88**, 021002 (2016).